Planar Circuits, Waveguide Models, and Segmentation Method

ROBERTO SORRENTINO, SENIOR MEMBER, IEEE

(Invited Paper)

Abstract **—The planar-circuit approach to the analysis and design of microwave integrated circuits (MIC's), with specific reference to microstrip circuits, is reviewed. The planar approach overcomes the limitations inherent to the more conventional transmission-line approach. As the operating frequency is increased and/or low-impedence levels are required, in fact, the transverse dimensions of the circuit elements become comparable with the wavelength and/or the longitudinal dimensions. In such cases, one-dimensional analyses give inaccurate or even erroneous results.**

The analysis of planar elements is formulated in terms of an N-port circuit and results in a generalized impedance-matrix description. Analysis techniques for simple geometries, such as the resonant mode expansion, and for more complicated planar configurations, such as the segmentation method, are discussed along with planar models for accounting for fringing fields effects and radiation loss.

I. Introduction

As MICROWAVE TECHNOLOGY evolves toward the use of higher frequencies and more sophisticated circuits and components, a considerable theoretical effort is required in order to improve the characterization and modeling of microwave structures. This is the basis for reliable computer-aided design (CAD) techniques.

In the setup of CAD techniques, one has to compromise between accuracy and simplicity. Exact analyses are often impractical because of the exceedingly high computer time required. From this viewpoint, the planar-circuit approach is a very powerful technique, which has been basically developed for the analysis of microstrip circuits, but can be extended to other microwave circuit configurations, such as reduced-height waveguide, stripline, suspended microstrip, etc.

Though the planar circuit is an approximate model of microstrip components, it constitutes a substantial improvement over conventional transmission-line models, providing accurate descriptions of their performances. On the other hand, planar-circuit models are simple enough to keep computer analyses reasonably inexpensive.

It is the scope of this paper to review the theoretical basis of the planar-circuit approach and to stress its suitability to the characterization, modeling, and design of two-dimensional microwave structures, with specific reference to microstrip circuits. This paper is not intended to provide details on planar-circuit analysis and design, which can be found in the referenced papers and overview books [1]–[3], but to illustrate the main features of the planar approach in contrast with the more conventional transmission-line approach.

The concept and definition of planar circuits are introduced in the next section, and the advantages of such an approach are briefly described. Starting from Maxwell's equations, the theoretical bases for the analysis of planar microwave components in terms of a two-dimensional circuit model are assessed in Section III. The terminal description of planar circuit is derived in Section IV; this is the basis for a brief discussion on the filtering properties and lumped-element equivalent circuits of planar elements. Once the terminal description of a single planar element has been obtained, the techniques mentioned in Section V, such as the segmentation method, can be applied to the analysis of more complicated planar configurations. The techniques for modeling a microstrip component such as a planar circuit, so as to account for effects of fringe fields and radiation loss, are discussed in Section VI. Finally, in order to describe the effects of planarity in microstrip circuits, a simple stub structure is taken as an example and its behavior illustrated in some detail in Section VII.

II. The Planar Circuit

The concept of a planar circuit was introduced by Okoshi and Miyoshi [4] as an approach to the analysis of microwave integrated circuits (MIC's). Depending on the number of dimensions which are comparable with the operating wavelength, conventional circuit elements can be classified into three categories: zero-dimensional (lumped), one-dimensional (uniform transmission lines), and three-dimensional (waveguides). The fourth category is represented by two-dimensional or planar circuits (Fig. 1). A planar circuit is defined as an electrical circuit having two dimensions comparable with the wavelength, while the third dimension is a negligible fraction of the wavelength. Strictly speaking, a distinction should be made between a microwave planar element and a planar circuit, the latter being the mathematical model, phrased in terms of voltage and current, of the former; in some instances throughout this paper, however, the two terms can be used indistinctly.

As will be shown in the next section, a two-dimensional circuit theory can be developed for planar components by extending to the two-dimensional case the concepts of

Manuscript received February 5, 1985; revised June 3, 1985.
The author is with the Department of Electronics, University of Rome La Sapienza, Rome, Italy.

0018-9480/85/1000-1057$01.00

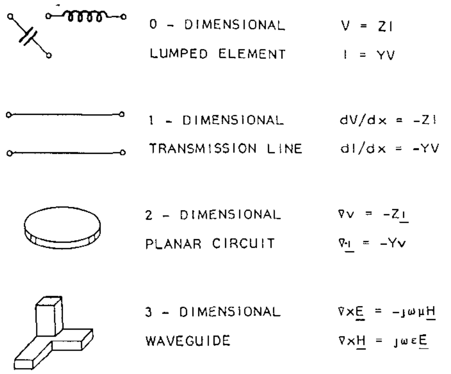

Fig 1. Classification of electrical components.

voltage and current usually defined in transmission-line theory.

The planar approach can be used to characterize a number of MIC components, basically in stripline or microstrip configuration, which typically have one dimension, the substrate thickness, much smaller than the operating wavelength. Our attention will be focused on microstrip circuits, which presently play a major role in the area of MIC's.

With reference to a microstrip component, it should be observed that it can be only approximately considered as a planar circuit, as the electromagnetic (EM) field is not entirely confined to the substrate region but, particularly near the edges of the metallization, extends into air outside the dielectric substrate. In other words, the presence of stray fields makes the planar-circuit concept not rigorously applicable to microstrip components. Nonetheless, as discussed in Section VI, provided suitable modifications in terms of effective parameters are made, planar models provide accurate enough characterizations of microstrip circuits and components.

The planar-circuit model is intermediate between transmission-line and full-wave three-dimensional models. In some respects, it combines advantages of both approaches. On the one hand, with respect to the usual transmission-line description of microstrip circuits, the planar description is far more accurate, while, on the other hand, it is much more simple and computationally affordable than a full-wave description.

The advantages associated with the planar-circuit approach can be summarized as follows.

1) The planar-circuit approach provides accurate descriptions of microstrip components and discontinuities. As the operating frequency is increased and low-impedance values are required, the performance of microstrip circuits designed on a transmission-line basis deteriorates because of unwanted reactances associated with discontinuities. The EM field cannot any longer be assumed to have a uniform distribution in the transverse direction so that a planar approach is required to obtain accurate characterizations of the circuit performances.

2) New classes of components can be analyzed and designed using the planar-circuit approach. The wider degree of freedom of planar elements can be used to obtain specific performances and to overcome the limitation inherent to the one-dimensional approach. Several new components have been designed which utilize the planar concept, such as 3-dB hybrid circuits [5], bias filter elements [6], coupled-mode filters [7], in-phase 3-dB power dividers [8], etc.; circular polarization in microstrip antennas is obtained exciting two degenerate orthogonal modes in a planar structure [9].

3) Planar circuits are simpler to analyze than three-dimensional circuits. Although a three-dimensional full-wave analysis is the only rigorous approach to characterize microstrip circuits and components, it is too laborious and computer time consuming for most practical purposes. Planar-circuit analyses, on the contrary, require reasonably short computer times, while providing descriptions which are generally accurate enough for the needs of the microstrip circuit designer.

III. Planar-Circuit Analysis

The basic equations for the analysis of N-port planar circuits are derived in this section. The case of magnetic wall boundaries is considered, as is usually assumed for representing a microstrip or stripline component. A terminal description in terms of an impedance matrix can be derived for this type of planar circuit. The case of electrically conducting boundaries, which is representative for reduced-height waveguide, can be treated in a similar manner and described in terms of an admittance matrix [11].

Fig. 2 shows a schematic of a N-port planar element. The EM field is confined by two parallel perfectly conducting plates (top and bottom) bounded by the contour $\mathscr{C}$ and, laterally, by a cylindrical magnetic-wall surface. The excitation of the EM field inside this structure may take place either through some apertures produced at the lateral wall to couple the planar element to the external circuit (edge-fed microstrip) or by some internal current sources J_z. The latter case is normally encountered only in antenna applications, while the former is the only one usually considered in MIC applications. Both cases, however, can be formally treated in the same way; it can be easily demonstrated, in fact, that the coupling aperture produced in the magnetic wall is equivalent to an electric-current density flowing on the aperture surface.

Because of planarity (thus $\partial/\partial z = 0$) and open-circuit boundary conditions, Maxwell's equations reduce to

$$\nabla_t E_z = -j\omega\mu\hat{z}\times \boldsymbol{H}_t \tag{1}$$

$$\nabla_t \times \boldsymbol{H}_t = (j\omega\epsilon E_z + J_z)\hat{z} \tag{2}$$

where ∇_t is the two-dimensional nabla operator, $\hat{z}$ is the unit vector normal to the plane of the circuit, μ and ϵ are the permeability and permittivity of the filling substrate material. The E-field has only the z-component, while the H-field lies in the xy plane.

A two-dimensional form of telegraphists' equations can be obtained from (1) and (2) defining at each point $\boldsymbol{r}$ of the planar circuit a voltage v and a surface current density $\boldsymbol{J}_s$

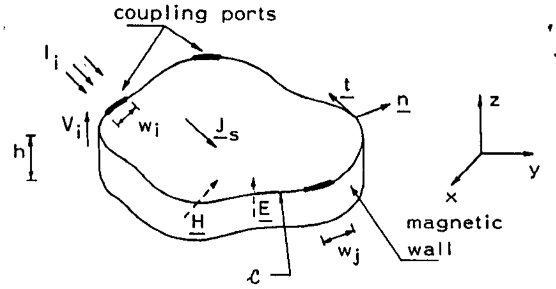

Fig. 2. Geometry of the planar circuit.

flowing on the top conductor as

$$v(\boldsymbol{r}) = -hE_z \qquad V \tag{3}$$

$$\boldsymbol{J}_s(\boldsymbol{r}) = -\hat{z} \times \boldsymbol{H}_t \qquad A/m \tag{4}$$

where h is the substrate thickness.

Note that the Poynting vector is given by

$$\boldsymbol{P} = \frac{1}{2}\boldsymbol{E} \times \boldsymbol{H}^* = \frac{1}{2h} v \boldsymbol{J}_s^* \qquad W/m^2$$

so that the quantity

$$\boldsymbol{P} = \frac{1}{2} v \boldsymbol{J}_s^* \qquad W/m$$

represents the linear power-density vector flowing on the planar circuit.

Inserting (3) and (4) into (1) and (2), we get

$$\nabla_t v = -j\omega\mu h \boldsymbol{J}_s \tag{5}$$

$$\nabla_t \cdot \boldsymbol{J}_s = -j\frac{\omega\epsilon}{h} v + J_z, \tag{6}$$

These equations represent a two-dimensional form of inhomogeneous telegraphists' equations, involving the voltage v and surface current density on the top metallic plate. The voltage wave equation is obtained taking the divergence of (5) and substituting into (6)

$$\nabla_t^2 v + k^2 v = -j\omega\mu h J_z \tag{7}$$

where

$$k^2 = \omega^2 \mu\epsilon.$$

The boundary condition associated with (7) is

$$\frac{\partial v}{\partial n} = \begin{cases} -j\omega\mu h \boldsymbol{J}_s \cdot \boldsymbol{n}, & \text{on } w_i,\ i = 1, 2, \cdots N \\ 0, & \text{elsewhere on } \mathscr{C} \end{cases} \tag{8}$$

w_i being the ith port of the planar circuit and $\boldsymbol{n}$ the outward directed normal to the periphery $\mathscr{C}$.

It can be demonstrated easily that the inhomogeneous boundary condition (8) can be replaced by a homogeneous boundary condition along the whole periphery $\mathscr{C}$, provided an additional equivalent current density

$$J_z = -\boldsymbol{J}_s \cdot \boldsymbol{n} \delta(\boldsymbol{r} - \boldsymbol{r}') \tag{9}$$

is assumed in (7), $\boldsymbol{r}'$ being the source location at w_i on the periphery $\mathscr{C}$.

A formal solution of (7) and (8) for the voltage v can be obtained using either the resonant-mode expansion technique [10], [11] or the Green's function approach [4]. The two approaches are substantially equivalent, since the Green's function is normally not known in closed form but is itself expressed in terms of a resonant mode expansion. In some cases, however, as discussed in Section VII, the Green's function approach can provide more compact analytical expressions leading to more efficient computer analyses. On the other hand, however, the resonant-mode technique provides a deeper physical insight, as it lends itself to a physical interpretation of the filtering properties of planar elements and is the basis for the modeling in terms of equivalent circuits.

The resonant-mode technique for planar structures with magnetic-wall boundaries can be obtained by suitably modifying the theory on field expansion in resonant cavities [12]. Let $\phi_\nu (\nu = 1, 2, \cdots)$ be the orthonormalized eigenfunctions of the following eigenvalue problem:

$$\begin{aligned} \nabla_t^2 \phi_\nu + k_\nu^2 \phi_\nu &= 0, \qquad \text{in } S \\ \frac{\partial \phi_\nu}{\partial n} &= 0, \qquad \text{on } \mathscr{C} \end{aligned} \tag{10}$$

where S is the planar region bounded by the contour $\mathscr{C}$. The lowest eigenvalue of (10) is $k_0^2 = 0$, corresponding to the electrostatic mode.

Once the set of eigenfunctions ϕ_ν is known, the solution of (7) can be expressed as

$$v(\boldsymbol{r}) = \sum_{\nu=0}^{\infty} A_\nu \phi_\nu \tag{11}$$

where

$$A_\nu = \frac{-j\omega\mu h}{k^2 - k_\nu^2} \int_S \phi_\nu J_z \, dS. \tag{12}$$

When the planar element is edge fed and no volume current sources are present inside it, because of (9), the integral over the planar surface S reduces to the integral over the ports at the periphery $\mathscr{C}$, so that (12) reduces to

$$A_\nu = \frac{-j\omega\mu h}{k^2 - k_\nu^2} \sum_{i=1}^{N} \int_{w_i} \boldsymbol{J}_s \cdot (-\boldsymbol{n}) \, dl. \tag{13}$$

The solution of (7) for a unit current density pulse δ located at $\boldsymbol{r}'$ gives the Green's function in terms of the set of eigenfunctions

$$G(\boldsymbol{r}, \boldsymbol{r}') = j\omega\mu h \sum_{\nu=0}^{\infty} \frac{\phi_\nu(\boldsymbol{r})\phi_\nu(\boldsymbol{r}')}{k_\nu^2 - k^2} \tag{14}$$

Using (14), the expression (11) for v can be replaced by

$$v(\boldsymbol{r}) = \int_S G(\boldsymbol{r}, \boldsymbol{r}') J_z(\boldsymbol{r}') \, dS \tag{15}$$

or, when (9) applies

$$v(\boldsymbol{r}) = \sum_{i=1}^{N} \int_{w_i} G(\boldsymbol{r}, \boldsymbol{r}')(-\boldsymbol{n} \cdot \boldsymbol{J}_s) \, dl. \tag{16}$$

It is worth noting that the Green's function is a frequency-dependent function, while eigenfunctions ϕ_ν are not. As a consequence, the frequency dependence of v is not apparent in (15) while it results in the form of a partial fraction expansion in (11) and (12).

IV. Terminal Description

From now on we shall assume the planar element to be edge fed, as in usual microstrip circuit applications.

Voltage and surface currents on the planar circuit are excited by a linear current density $-\boldsymbol{n}\cdot\boldsymbol{J}_s$ injected through the various ports. At the ith port, these quantities can be expressed by their Fourier expansions

$$v=\sum_{m=0}^{\infty} V_i^{(m)}\sqrt{\delta_m}\cos\frac{m\pi l}{w_i} \tag{17}$$

$$-\boldsymbol{n}\cdot\boldsymbol{J}_s=\sum_{n=0}^{\infty} J_i^{(n)}\sqrt{\delta_n}\cos\frac{n\pi l}{w_i} \tag{18}$$

where l is the coordinate along the ith port $(0\leqslant l\leqslant w_i)$, w_i the port width, δ_m the Neumann delta ($\delta_m=1$ for $m=0$, $\delta_m=2$ for $m\neq 0$). If the port is terminated by a transmission line having the same width w_i, $V_i^{(n)}$ and $J_i^{(n)}$ represent voltage and longitudinal current density amplitudes of the mode of nth order, $n=0$ being the dominant TEM mode. The voltage v and the current density entering the ith port, $-\boldsymbol{n}\cdot\boldsymbol{J}_s$, can be thus represented by their Fourier expansion coefficients

$$V_i^{(m)}=\frac{\sqrt{\delta_m}}{w_i}\int_{w_i} v\cos\frac{m\pi l}{w_i}\,dl \tag{19}$$

$$J_i^{(n)}=\frac{\sqrt{\delta_n}}{w_i}\int_{w_i}(-\boldsymbol{n}\cdot\boldsymbol{J}_s)\cos\frac{n\pi l}{w_i}\,dl. \tag{20}$$

The above definitions are such that the complex power entering the circuit through the ith port is given by

$$P_i=\frac{1}{2}\int_{w_i}\boldsymbol{E}\times\boldsymbol{H}^*\cdot(-\boldsymbol{n})\,dl=\frac{1}{2}\sum_{m=0}^{\infty}V_i^{(m)}I_i^{(m)*} \tag{21}$$

where we have defined

$$I_i^{(m)}=w_iJ_i^{(m)} \tag{22}$$

as the current entering the ith port associated with the mth order mode.

Inserting (11) and (13) into (19) and using (18) and (22), the relationship between voltage and currents is obtained in terms of the generalized impedance matrix of the planar circuit

$$V_i^{(m)}=\sum_{n=0}^{\infty}\sum_{j=1}^{N}Z_{ij}^{(mn)}I_j^{(n)} \tag{23}$$

where

$$Z_{ij}^{(mn)}=\frac{j\omega\mu h\sqrt{\delta_m\delta_n}}{w_iw_j}\sum_{\nu=0}^{\infty}\frac{g_{\nu i}^{(m)}g_{\nu j}^{(n)}}{k_\nu^2-k^2} \tag{24}$$

$$g_{\nu i}^{(m)}=\int_{w_i}\phi_\nu\cos\frac{m\pi l}{w_i}\,dl \tag{25}$$

$Z_{ij}^{(mn)}$ gives the mth order voltage at the ith port due to a unit nth order current injected at the jth port, all other currents being zero. With this procedure, each physical port corresponds to an infinite number of electrical ports, relative to the spatial harmonics of voltage and current. In practice, only a few terms of expansions (17) and (18) are required to represent with good approximation the voltage and current distributions along the ports. In most cases, the width w_i of the port is much smaller than both the wavelength and the dimensions of the circuit, so that only the 0th order terms need to be retained in (17) and (18).

A formally more compact expression for the Z-elements is obtained using the Green's function

$$Z_{ij}^{(mn)}=\frac{\sqrt{\delta_m\delta_n}}{w_iw_j}\int_{w_i}dl\int_{w_j}G(\boldsymbol{r},\boldsymbol{r}')\cos\frac{m\pi l}{w_i}\cos\frac{n\pi l'}{w_j}\,dl'. \tag{26}$$

Expression (24), or (26), forms the basis for the description of the microwave planar element as an electrical circuit. Descriptions in terms of a generalized scattering matrix can be easily obtained through known formulas.

It is worth noting that the frequency dependence of the Z-parameters is not apparent in (26), as it is incorporated in the Green's function. Since coefficients (25) are frequency independent, on the contrary, the partial fraction expansion (24) explicitly shows the frequency dependence of the impedance parameters. Expression (24) is therefore useful to interpret the filtering properties of planar circuits and lends itself to the evaluation of equivalent-lumped circuits. These aspects are briefly discussed herein in the case of two-port ($N=2$) planar elements.

As mentioned above, a notable simplification can be made when, as in many practical circuits, the ports are very narrow with respect to both the wavelength and the dimensions of the planar element. In such cases, the contribution of higher order modes ($n\geqslant 1$) at the ports can be neglected, so that voltages and current densities are assumed to be constant along the ports. For two-port elements, the Z-matrix reduces to a 2×2 matrix relating the voltages and currents of the dominant (0th order) modes at the two ports. Omitting for simplicity the indexes $m=n=0$, (24) and (25) become

$$Z_{ij}=\frac{j\omega h}{w_iw_j\epsilon}\sum_{\nu=0}^{\infty}\frac{g_{\nu i}g_{\nu j}}{\omega_\nu^2-\omega^2} \tag{27}$$

$$g_{\nu i}=\int_{w_i}\phi_\nu\,dl \tag{28}$$

where we have put $k_\nu^2=\omega_\nu^2\mu\epsilon$ and $k^2=\omega^2\mu\epsilon$. The above expressions can be used to obtain a general equivalent-lumped circuit in the form of a series connection, through ideal transformers, of anti-resonant LC cells, each cell corresponding to a resonant mode of the structure. If the planar element is symmetrical, then $|g_{\nu 1}|=|g_{\nu 2}|$, and the equivalent circuit can be put in the form of a symmetrical lattice network without any use of transformers [13].

For practical applications, only a finite number of cells are to be included in the equivalent circuit; such a number depends on the frequency range of interest and on the approximation required. In a low-frequency approximation, only the first two resonant modes can be taken into account, i.e., the static mode resonating at zero frequency and the first higher mode. When the latter is an odd mode, it can be easily shown that the equivalent circuit has the same structure as a third-order elliptic filter [14]. On this basis, low-pass filters with elliptic function responses have been designed by cascading microstrip rectangular elements [15].

The physical nature of the transmission zeros occurring in planar circuits can be easily interpreted on the basis of (27) [10]. It is well known that transmission zeros ($s_{21}=0$) in two-port networks occur in two cases: a) for $Z_{21}=0$ and b) for Z_{21} finite and Z_{11} or Z_{22} infinite. For planar elements, the latter case can occur at some specific resonant frequencies of the structure. This type of transmission zero has been called a modal transmission zero and occurs when a resonant mode 'ν' can be excited from one port ($g_{\nu 1} \neq 0$), but is uncoupled to the other port ($g_{\nu 2}=0$). The former type of transmission zero ($Z_{21}=0$), on the contrary, is due to the destructive interaction between resonant modes. While the frequency location of a modal transmission zero is determined only by the shape and dimensions of the planar element, the frequency location of an interaction transmission zero can be controlled by varying the position of the ports [6].

The same distinction between transmission zeros applies to waveguide circuits and has been used to improve selectivity in cylindrical filters [16]. A liquid-crystal field mapping technique for MIC's [17], [18] can been used to give perceptible evidence to these results [19].

V. Segmentation of Planar Elements

Numerical techniques [1], [4], [21], [22], [47], should be used for the analysis of planar elements with completely arbitrary shapes. Eigenfunctions ϕ_ν and Green's function G, in fact, are known for a limited number of simple geometrical shapes, such as rectangles, circles, circular sectors, rings, and annular sectors, etc. A number of Green's functions for such and other simple shapes are listed in [2] and [20].

The analysis of planar elements, however, can be easily extended to those geometries which result from the connection of elementary shapes. This is illustrated in a simple example. The structure of Fig. 3 can be decomposed into the cascade of two subelements (Fig. 3(b)) for which the impedance matrices $[Z_a]$ and $[Z_b]$ can be computed as discussed in the previous section. By grouping together voltages and currents at the connected ports, $[Z_a]$ and $[Z_b]$ can be put in the form

$$[Z_a]=\begin{bmatrix}[Z_{a11}] & [Z_{a12}]\\ [Z_{a21}] & [Z_{a22}]\end{bmatrix} \quad [Z_b]=\begin{bmatrix}[Z_{b11}] & [Z_{b12}]\\ [Z_{b21}] & [Z_{b22}]\end{bmatrix}. \tag{29}$$

Using the conditions imposed by the cascade connection, i.e.,

$$[V_{a2}]=[V_{b1}] \quad [I_{a2}]=-[I_{b1}] \tag{30}$$

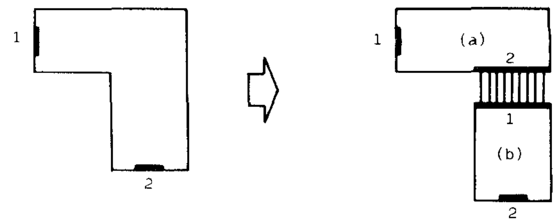

Fig. 3. Segmentation of planar elements.

the Z-matrix of the resulting network is expressed by

$$[Z]=\begin{bmatrix}[Z_{11}] & [Z_{12}]\\ [Z_{21}] & [Z_{22}]\end{bmatrix}$$

$$\begin{aligned}[Z_{11}]&=[Z_{a11}]-[Z_{a12}][Y_{ab}][Z_{a21}]\\ [Z_{12}]&=[Z_{a12}][Y_{ab}][Z_{b12}]\\ [Z_{21}]&=[Z_{b21}][Y_{ab}][Z_{a21}]\\ [Z_{22}]&=[Z_{b22}]-[Z_{b21}][Y_{ab}][Z_{b12}]\end{aligned} \tag{31}$$

where

$$[Y_{ab}]=([Z_{a22}]+[Z_{b11}])^{-1}. \tag{32}$$

Note that, according to the technique described in the previous section, voltage and current distributions at the interconnection between the planar elements are expressed in terms of their Fourier expansions, so that the same physical port corresponds to different (infinite, in theory) electrical ports. In practice, voltage and currents are approximated by truncated Fourier expansions, corresponding to a finite number of electrical ports.

An alternative technique is the segmentation method, in which, on the contrary, the interconnection is discretized into a finite number of ports. Voltage and current are assumed to be constant along each port, which thus corresponds to one electrical port. Voltage and current distributions along the interconnection are so approximated by stepped functions. The segmentation method has been originally formulated in terms of scattering matrix [23], but can be also implemented with higher computational efficiency in terms of impedance matrices [24].

The analysis of complicated geometries can be further extended by the desegmentation method [25], [26]. This technique can be applied to those geometries which, after addition of a simple element, can be analyzed by either the elementary or segmentation methods. In other words, the desegmentation method applies to geometries resulting from the subtraction of a simple shape from another geometry which can be analyzed by segmentation.

VI. Planar Models of Microstrip Circuits

As previously mentioned, a microstrip circuit cannot be considered as a planar circuit but only in an approximate way. Substantial discrepancies may arise due to the fields at the edges of the metallization. Nevertheless, an equivalent planar circuit can be used to model the microstrip circuit. This section will discuss how to define such an equivalent planar model.

As is known, the dynamic properties of a uniform microstripline can be calculated using an equivalent planar waveguide model [27], [28]. This is a waveguide with lateral magnetic walls, having the same height h as the substrate thickness. The width w_e and the permittivity of the filling dielectric are determined by the conditions that both the phase velocity and the characteristic impedance be the same as for the microstripline. As the dominant mode of the planar waveguide is a TEM mode, the equality of the phase velocities imposes that the filling dielectric has the same effective permittivity ϵ_e of the quasi-TEM mode of the microstripline, while the condition on the characteristic impedance imposes that

$$Z_0 = \eta_o h / \left(w_e \sqrt{\epsilon}_e \right)$$

where Z_0 is the characteristic impedance defined for the microstripline, $\eta_0 = \sqrt{\mu_0/\epsilon_0}$ is the free-space impedance. A frequency dependence of ϵ_e and w_e can be introduced to account for dispersion on the phase velocity and characteristic impedance [28].

The planar waveguide model has been found to provide a good approximation of the cutoff frequencies of higher order modes of the microstripline. The usefulness of this model relies on the reduction of an open structure into a closed one; it therefore substantially simplifies the calculation of microstrip discontinuities. In some sense, the planar waveguide is a two-dimensional model, as it takes into account the transverse variations of the EM field. This model has found a number of applications from the analysis of the frequency-dependent properties of microstrip discontinuities [29], [30] to the design of stepped microstrip components [31], microstrip power dividers [32], and computer-aided design of microstrip filters [33].

It seems reasonable to extend the planar waveguide model to the case of two-dimensional microstrip circuits using a planar circuit with effective dimensions and an effective permittivity. The case of two-dimensional elements, however, is more complicated, as the EM field is allowed to vary along two directions. To illustrate this point with an example, let us consider the case of a two-port circular microstrip. Fig. 4(a) shows the experimental frequency behavior of the scattering parameter $|s_{21}|$. The theoretical behavior of Fig. 4(b) has been obtained by applying the mode expansion technique and by suitably choosing the effective parameters of the circular microstrip so as to optimize the agreement with Fig. 4(a).

A good agreement between theory and experiment is observed up to ~12 GHz. Above this frequency, the theory appears to be inconsistent with the experiment. Such an inconsistency can be explained by the following argument.

The effective permittivity is used to account for the electric-field lines being more or less confined to the substrate material and therefore depends on the electric-field distribution along the edge of the planar element. Considering the EM field as the superposition of the resonant modes of the structure, it is evident that a different effective permittivity should be ascribed to resonant modes having a different field distribution along the periphery of the circuit.

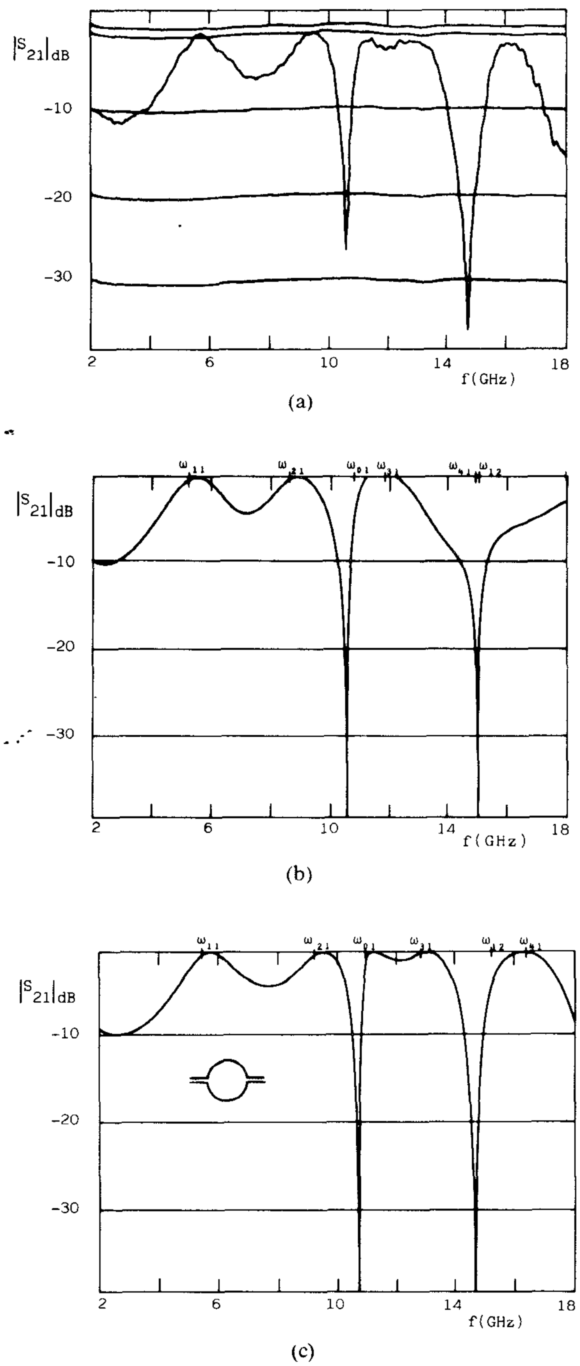

Fig. 4. Scattering parameter $|s_{21}|$ of a circular microstrip. (a) Experiment (after [10]). (b) Theoretical analysis using a single effective model. (c) Theoretical analysis using a different effective model for each resonant mode (after [10]).

Wolff and Knoppik have developed a theory [34] for computing the resonant frequencies of circular and rectangular microstrip resonators using a planar model. The theory can be extended to ring resonators [35]–[37]. This model is characterized by effective dimensions and effective permittivities which depend on the resonant mode; it can be used in conjunction with the resonant-mode technique to get the results of Fig. 4(c) [7]. The agreement with the experiment of Fig. 4(a) is quite good up to 18 GHz. The comparison between Fig. 4(b) and (c) shows that each resonant frequency undergoes a different shift; in particular, the resonant frequencies ω_{14} and ω_{21} are interchanged.

This example demonstrates that an accurate characterization of a two-dimensional microstrip circuit can be achieved through an effective planar-circuit model in conjunction with the resonant-mode technique, provided a suitable effective permittivity is used for each resonant mode. The effective permittivity accounts for the reactive energy associated with the fringing field of the corresponding mode and may produce modal inversions. Since, as previously demonstrated, the response of a planar element is tightly related to the sequence of resonant modes, the alteration of that sequence produces strong alterations of the frequency behavior of the circuit.

An additional source of discrepancy may be due to radiation loss. Differently from dielectric and conductor losses, which are associated with the field distribution inside the microstrip element, radiation loss depends on the field distribution along the periphery of the circuit. Conductor and dielectric losses do not alter substantially the circuit performance, but usually only introduce some degradations. On the contrary, radiation loss may produce effects substantially different from those predicted on the basis of a lossless theory.

A typical example is represented by nonsymmetrical structures. For a lossless reciprocal two-port network, $|s_{11}| = |s_{22}|$ at any frequency; this equality is no longer valid in the presence of losses. It has been experimentally observed in nonsymmetrical rectangular microstrips, in fact, that at some particular frequencies $|s_{11}| \cong 0$ while $|s_{22}| \cong 1$ [41]. This phenomenon occurs when a resonant mode, which strongly radiates, can be excited from the first port, but is uncoupled with the second one.

An exact theory for calculating radiation loss from microstrip structures has not been developed. The resonant-mode technique applied to planar circuits, however, can be extended to include radiation loss in an approximate way. This technique, in fact, has been extensively applied to the analysis of microstrip antennas [9], [38]–[40]. Basically, one has to account for radiation by assuming that the tangential magnetic field at the periphery of the circuit is different from zero, so that the field expansion coefficients must be modified accordingly. The general formulation presented in [41] is of impractical use; neglecting the coupling between resonant modes, which arises from the inhomogeneous boundary conditions, a simplified theory can be derived which reduces the problem to the evaluation of the complex power radiated by each unperturbed resonant mode. In spite of the approximations involved, which include neglecting surface waves, this theory was shown to accurately predict in a quantitative way the frequency behavior of the scattering parameters of rectangular and circular microstrip structures.

VII. Planar Analysis of Stub Structure

The limitations of the transmission-line (one-dimensional) approach to the analysis and design of MIC's are illustrated and discussed in this section, through the simple but typical and significant example of a stub structure.

The stub is used to provide a zero-impedance level, thus a transmission zero, at the frequency corresponding to a quarter of wavelength. Low-characteristic impedances of the stub are required for broad-band applications, so that, in microstrip circuits, this function is more conveniently realized as the parallel of two stubs. We are therefore led to the consideration of the double-stub structure of Fig. 5.

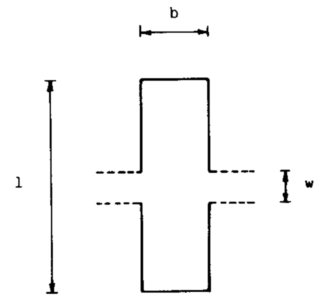

Fig. 5. Geometry of a double stub.

From a planar point of view, this is a rectangular element $b \times l$ symmetrically connected to a main line of width w. With reference to the discussion of Section VI on fringe field effects, a different effective model should be used for each resonant mode of the structure. In order to simplify the discussion, which is aimed to point out two-dimensional effects arising even in a simplified model independently of fringe field effects, this structure will be characterized by a unique effective model, i.e., by effective dimensions w_e, b_e, l_e and effective dielectric constant ϵ_e. (This is a planar waveguide model, which is strictly valid as long as $l_e > b_e$ and higher order modes excited at the connection with the main line are rapidly decaying toward the open ends of the stub structure.)

Depending on the dimensions and the frequency range, the rectangular structure behaves as: a) a shunt capacitor $C = \epsilon_e l_e b_e / h$ in the limit of very low frequencies, so that $w_e, b_e, l_e \ll \lambda$; b) a shunt stub of transmission line with characteristic impedance $Z_0/2 = (1/2) h\eta_0 / (b_e\sqrt{\epsilon_e})$ and length $l_e/2$ as long as $w_e, b_e \ll \lambda$ and $w_e \ll l_e$; c) a planar circuit in all other cases.

The general case c), which includes a) and b) as special cases, can be treated as in Section III by evaluating the generalized impedance matrix, which accounts also for reflected and transmitted higher order modes on the main line. If these modes are evanescent and the line is long enough at both ends so that the discontinuity represented by the stub does not interact with other possible discontinuities, higher order modes have a negligible effect. In such a case, the Z-matrix computation can be reduced to the only terms relative to the dominant modes ($m = n = 0$ in (24)).

Using the resonant-mode technique, the Z-matrix is expressed in the form of a double series over indexes r and s corresponding to the resonances along l and b, respectively. More specifically, one obtains

$$Z_{11} = Z_{22} = j\omega c Z_0 \sum_{r=0}^{\infty} \sum_{s=0}^{\infty} \frac{g_{rs}^2}{\omega_{rs}^2 - \omega^2}$$

$$Z_{12} = Z_{21} = j\omega c Z_0 \sum_{r=0}^{\infty} \sum_{s=0}^{\infty} \frac{(-1)^s g_{rs}^2}{\omega_{rs}^2 - \omega^2} \qquad (33)$$

with

$$c = 1/\sqrt{\mu_0 \epsilon_0 \epsilon_e}$$

$$Z_0 = \frac{h}{b_e} \eta_0 / \sqrt{\epsilon_e}$$

$$\omega_{rs} = c\sqrt{(r\pi/l_e)^2 + (s\pi/b_e)^2}$$

$$g_{rs} = \sqrt{\frac{\delta_r \delta_s}{l_e}} \operatorname{sinc}\left(\frac{r\pi w_e}{2l_e}\right) \cos \frac{r\pi}{2}. \tag{34}$$

In the numerical computation of the Z-parameters, it would be convenient to evaluate analytically the series in (33). Actually, it could be shown that either the series over r or that over s can be expressed in a closed form. This can be done by regarding the rectangular structure as a section of planar waveguide with its longitudinal axis directed along either the length l or the width b, respectively. In both cases, the Green's function is obtained as a single series involving the modes of the planar waveguide. It is found, in particular, that (33)–(34) can be replaced by

$$Z_{11} = Z_{22} = j \sum_{s=0}^{\infty} X_s \quad Z_{12} = Z_{21} = j \sum_{s=0}^{\infty} (-1)^s X_s \tag{35}$$

with

$$X_s = -Z_0 \cdot \frac{\beta_0}{\beta_s} \delta_s \left[\frac{1}{2} \operatorname{cotan}\left(\frac{\beta_s l_e}{2}\right) \operatorname{sinc}^2\left(\frac{\beta_s w_e}{2}\right) + \frac{\beta_s w_e - \sin(\beta_s w_e)}{(\beta_s w_e)^2} \right] \tag{36}$$

$$\beta_s^2 = \omega^2 \mu \epsilon_0 \epsilon_e - (s\pi/b_e)^2.$$

Trigonometric functions in (36) reduce to corresponding hyperbolic functions when the frequency and the index s are such that $\beta_s^2 < 0$. This corresponds to the sth order mode being below cutoff. Clearly, (35) and (36) are computationally much more efficient than (33) and (34). Alternative expressions can be obtained by evaluating analytically the series over s in (33) [42], [43]. In such a case, the rectangular structure is viewed as a longitudinally symmetric cascade of two step discontinuities.

Expressions (35) and (36) permit one to point out the differences between the planar approach and the transmission-line approach; they reduce to the usual expressions for the parallel of two shunt open stubs: a) retaining only the 0th order terms in (35) and b) in the limit for $w_e/\lambda \to 0$

$$\lim X_0 = \frac{Z_0}{2} \operatorname{cotan}\left(\frac{\beta_0 l_e}{2}\right).$$

It is worth noting that discrepancies between planar and transmission-line models arise not only because of the excitation of higher order modes ($s > 0$) in the stub structure, but also because of the finite width w_e of the ports. Even if the stub has a high characteristic impedance, and higher order modes can therefore be neglected, in fact, the finite width of the ports produces both a shift of the zero impedance frequency f_0 (because of the additive term appearing in (36)), and a different impedance slope (because of the coefficient of the cotangent).

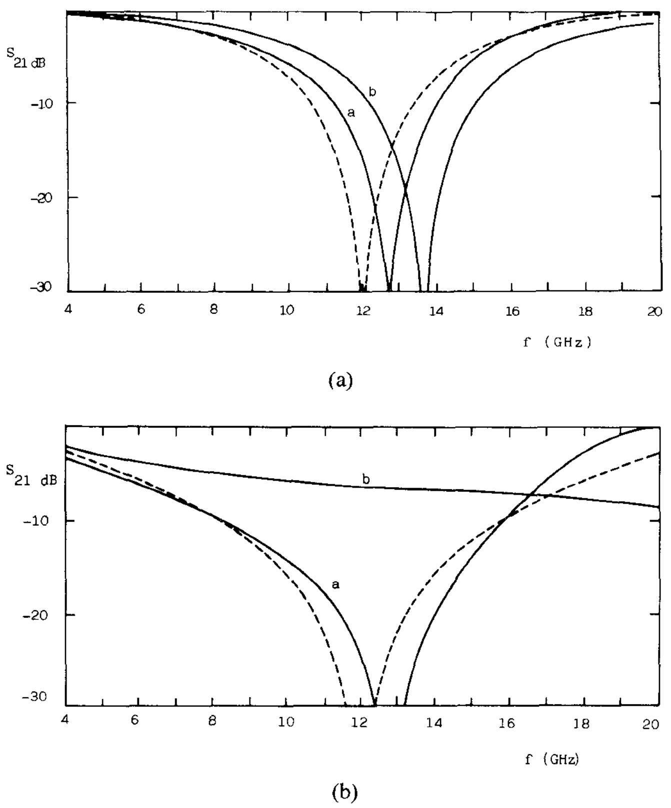

Fig. 6. (a) Scattering parameter $|s_{21}|$ of a double stub with $Z_0 = 90$ Ω, $f_0 = 12$ GHz: ideal response (dashed line); a planar analysis neglecting higher mode and b with higher modes. (b) Same as Fig. 6(a), but with $Z_0 = 30$ Ω.

These effects are illustrated in Fig. 6(a) and (b). Fig. 6(a) shows the frequency behavior of the scattering parameter $|s_{21}|$ of a double stub with $Z_0 = 90$ Ω inserted on a 50-Ω line. The length of the stub has been chosen so that $(l_e - w_e) = \lambda/2$ at the frequency $f_0 = 12$ GHz. The dotted curve represents the response obtained by an ideal transmission-line model. Curve a has been computed including in (35) only the 0th order terms. A notable shift of the transmission zero frequency is observed because of the finite width of the 50-Ω line. The inclusion of higher order terms in (35), curve (b), gives rise to a further shift of the frequency f_0, which is about 13.7 GHz instead of 12 GHz.

These effects become even more marked if the stub impedance is reduced. Because of the excitation of higher order modes, the transmission zero may eventually disappear, as shown in Fig. 6(b), where the double stub impedance has been chosen as 30 Ω.

The difficulties of designing microstrip stubs with low-characteristic impedances have suggested the use of alternative structures, such as radial line stubs [44]–[46]. Linear stubs, however, can still be used, provided a planar approach is used in the design. This is demonstrated in Fig. 7, where the response of the planar structure designed is compared with that of an ideal transmission-line single stub of 15 Ω. Although the rectangular structure exhibits a somewhat more selective behavior, nevertheless the response appears to be satisfactory for practical applications. This simple example shows the wider design possibilities of the planar approach, which permits one to overcome the limitations inherent to the one-dimensional approach.

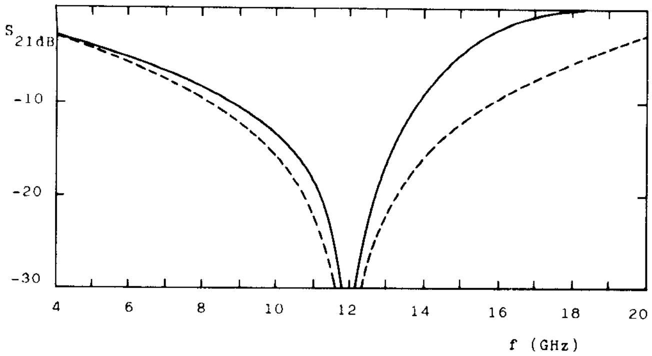

Fig. 7. Behavior of a planar stub designed to have a transmission zero at $f_0 = 12$ GHz, compared with the ideal response of a 15-Ω stub (----.)

VIII. Conclusion

An attempt has been made to review the planar-circuit concept and its theoretical basis for analysis and design of microwave planar components.

It has been stressed that the planar approach to MIC's is an approximate technique and therefore cannot be expected to provide extremely accurate results in all actual problems: to this scope, hybrid-mode full-wave techniques should be used. In conjunction with the planar models discussed in Section VI, however, accurate characterizations are obtained in most practical cases, including radiation loss, in such a way as to overcome the limitations inherent to the conventional transmission-line approach in the analysis and design of MIC's.

Acknowledgment

Since 1976, most of the work the author has done in the area of MIC's has been promoted and encouraged by Prof. F. Giannini. Prof. M. Salerno is gratefully acknowledged for helpful discussions.

References

[1] K. C. Gupta *et al.*, *Microstriplines and Slotlines*, Dedham, MA: Artech House, 1979.
[2] K. C. Gupta *et al.*, *Computer-Aided Design of Microwave Circuits*, Dedham, MA: Artech House, 1981.
[3] T. C. Edwards, *Foundations for Microstrip Circuit Design*, New York: Wiley, 1981.
[4] T. Okoshi and T. Miyoshi, "The planar circuit—An approach to microwave integrated circuitry," *IEEE Trans. Microwave Theory Tech.*, vol. MTT-20, pp. 245–252, 1972.
[5] T. Okoshi, T. Takeuchi, and J. P. Hsu, "Planar 3-dB hybrid circuit," *Electronics Comm. Japan*, vol. 58-B, pp. 80–90, 1975.
[6] G. D'Inzeo, F. Giannini, and R. Sorrentino, "Design of circular planar networks for bias filter elements in microwave integrated circuits," *Alta Freq.*, vol. 48, pp 251e–257e, July 1979.
[7] T. Miyoshi and T. Okoshi, "Analysis of microwave planar circuits," *Electronics Comm. Japan*, vol. 55-B, pp. 24–31, 1972.
[8] K. C. Gupta, R. Chadha, and P. C. Sharma, "Two-dimensional analysis for stripline microstrip circuits," *IEEE MTT-S Int. Microwave Symp. Dig.* (Los Angeles), 1981, pp. 504–506.
[9] K. R. Carver and J. W. Mink, "Microstrip antenna technology," *IEEE Trans. Antennas Propagat.*, vol. AP-29, pp. 2–24, Jan. 1981.
[10] G. D'Inzeo, F. Giannini, C. M. Sodi, and R. Sorrentino, "Method of analysis and filtering properties of microwave planar networks," *IEEE Trans. Microwave Theory Tech.*, vol. MTT-26, pp. 462–471, July 1978.
[11] P. P. Civalleri and S. Ridella, "Impedance and admittance matrices of distributed three-layer *N*-ports," *IEEE Trans. Circuit Theory*, vol. CT-17, pp. 392–398, Aug. 1970.
[12] K. Kurokawa, *An Introduction to the Theory of Microwave Circuits.* New York: Academic Press, 1967, ch. 4.
[13] G. D'Inzeo, F. Giannini, and R. Sorrentino, "Wide-band equivalent circuits of microwave planar networks," *IEEE Trans. Microwave Theory Tech.*, vol. MTT-24, pp. 1107–1113, Oct. 1980.
[14] G. D'Inzeo, F. Giannini, and R. Sorrentino, "Novel integrated low-pass filter," *Electron. Lett.*, vol. 15, pp. 258–260, Apr. 1979.
[15] F. Giannini, M. Salerno, and R. Sorrentino, "Design of low-pass elliptic filters by means of cascaded microstrip rectangular elements," *IEEE Trans. Microwave Theory Tech.*, vol. MTT-30, pp. 1348–1353, Sept. 1982.
[16] D. E. Kreinheder and T. D. Lingren, "Improved selectivity in cylindrical TE_{011} filters by TE_{211}/TE_{311} mode control," *IEEE Trans. Microwave Theory Tech.*, vol. MTT-30, pp. 1383–1387, Sept. 1982.
[17] F. Giannini, P. Maltese, and R. Sorrentino, "Liquid crystal technique for field detection in microwave integrated circuitry," *Alta Freq.*, vol. 46, pp. 80e–88E, Apr. 1977.
[18] F. Giannini, P. Maltese, and R. Sorrentino, "Liquid crystal improved technique for thermal field measurements," *Appl. Opt.*, vol. 18, no. 17, pp. 3048–3052, Sept. 1979.
[19] G. D'Inzeo, F. Giannini, P. Maltese, and R. Sorrentino, "On the double nature of transmission zeros in microstrip structures," *Proc. IEEE*, vol. 66, pp. 800–802, July 1978.
[20] K. C. Gupta, "Two-dimensional analysis of microstrip circuits and antennae," *J. Inst. Electronics Telecomm. Engrs.*, vol. 28, pp. 346-364, July 1982.
[21] P. Silvester, "Finite element analysis of planar microwave circuits," *IEEE Trans. Microwave Theory Tech.*, vol. MTT-21, pp. 104–108, Feb. 1973.
[22] G. D'Inzeo, F. Giannini, and R. Sorrentino, "Theoretical and experimental analysis of non-uniform microstrip lines in the frequency range 2–18 GHz," in *Proc. 6th Euro. Microwave Conf.*, 1976, pp. 627–631.
[23] T. Okoshi, Y. Uehara, and T. Takeuchi, "The segmentation method—An approach to the analysis of microwave planar circuits," *IEEE Trans. Microwave Theory Tech.*, vol. MTT-24, pp. 662–668, Oct. 1976.
[24] R. Chadha and K. C. Gupta, "Segmentation method using impedance matrices for analysis of planar microwave circuits," *IEEE Trans. Microwave Theory Tech.*, vol. MTT-29, pp. 71–74, Jan. 1981.
[25] P. C. Sharma and K. C. Gupta, "Desegmentation method for analysis of two-dimensional microwave circuits," *IEEE Trans. Microwave Theory Tech.*, vol. MTT-29, pp. 1094–1097, 1981.
[26] P. C. Sharma and K. C. Gupta, "An alternative procedure for implementing the desegmentation method," *IEEE Trans. Microwave Theory Tech.*, vol. MTT-32, pp. 1–4, Jan. 1984.
[27] I. Wolff, G. Kompa, and R. Mehran, "Calculation method for microstrip discontinuities and T-junctions," *Electron. Lett.*, vol. 8, pp. 177–179, Apr. 1972.
[28] G. Kompa and R. Mehran, "Planar waveguide model for calculating microstrip components," *Electron. Lett.*, vol. 11, pp. 459–460, Sept. 1975.
[29] G. Kompa, "*S*-matrix computation of microstrip discontinuities with a planar waveguide model," *Arch. Elek. Übertragung.*, vol. 30, pp. 58–64, Feb. 1976.
[30] W. Menzel and I. Wolff, "A method for calculating the frequency-dependent properties of microstrip discontinuities," *IEEE Trans. Microwave Theory Tech.*, vol. MTT-25, pp. 107–112, Feb. 1977.
[31] G. Kompa, "Design of stepped microstrip components," *Radio Electron. Eng.*, vol. 48, pp. 53–63, Jan./Feb. 1978.
[32] W. Menzel, "Design of microstrip power dividers with simple geometry," *Electron. Lett.*, vol. 12, no. 24, pp. 639–640, Nov. 1976.
[33] R. Mehran, "Computer-aided design of microstrip filters considering dispersion, loss and discontinuity effects," *IEEE Trans. Microwave Theory Tech.*, vol. MTT-27, pp. 239–245, Mar. 1978.
[34] I. Wolff and N. Knoppik, "Rectangular and circular microstrip disk capacitors and resonators," *IEEE Trans. Microwave Theory Tech.*, vol. MTT-22, pp. 857–864, Oct. 1974.
[35] G. D'Inzeo, F. Giannini, R. Sorrentino, and J. Vrba, "Microwave planar networks: The annular structure," *Electron. Lett.*, vol. 14, no. 16, pp. 526–528, Aug. 1978.
[36] J. Vrba, "Dynamic permittivity of microstrip ring resonator," *Electron. Lett.*, vol. 15, no. 16, pp. 504–505, Aug. 1979.
[37] I Wolff and V. K. Tripathi, "The microstrip open-ring resonator," *IEEE Trans. Microwave Theory Tech.*, vol. MTT-32, pp. 102–107, Jan. 1984.
[38] K. R. Carver, "A modal expansion theory for the microstrip antenna," in *AP-S Int. Symp. Dig.*, vol. I, June 1979, pp. 101–104.

[39] A. G. Derneryd and A. G. Lind, "Cavity model of the rectangular microstrip antenna," *IEEE Trans. Antennas Propagat.*, vol. AP-27, pp. 12-1/12-11, Oct. 1979.
[40] Y. T. Lo, D. Solomon, and W. F. Richards, "Theory and experiment on microstrip antennas," *IEEE Trans. Antennas Propagat.*, vol. AP-27, pp. 137–145, Mar. 1979.
[41] R. Sorrentino and S. Pileri, "Method of analysis of planar networks including radiation loss," *IEEE Trans. Microwave Theory Tech.*, vol. MTT-29, pp. 942–948, Sept. 1981.
[42] B. Bianco and S. Ridella, "Nonconventional transmission zeros in distributed rectangular structures," *IEEE Trans. Microwave Theory Tech.*, vol. MTT-20, pp. 297–303, May 1972.
[43] B. Bianco, M. Granara, and S. Ridella, "Filtering properties of two-dimensional lines' discontinuities," *Alta Freq.*, vol. 42, pp. 140E–148E, June 1973.
[44] J. P. Vinding, "Radial line stubs as elements in strip line circuits," in *NEREM Rec.*, 1967, pp. 108–109.
[45] A. H. Atwater, "Microstrip reactive circuit elements," *IEEE Trans. Microwave Theory Tech.*, vol. MTT-31, pp. 488–491, June 1983.
[46] F. Giannini, R. Sorrentino, and J. Vrba, "Planar circuit analysis of microstrip radial stub," *IEEE Trans. Microwave Theory Tech.*, vol. MTT-32, pp. 1652–1655, Dec. 1984.
[47] E. Tonye and H. Baudrand, "Multimode *S*-parameters of planar multiport junctions by boundary element method," *Electron. Lett.*, vol. 20, no. 19, pp. 799–802, Sept. 1984.

Roberto Sorrentino (M'77–SM'84) received the Laurea degree in electronic engineering from the University of Rome La Sapienza, Rome, Italy, in 1971.

He then joined the Institute of Electronics of the same university under a fellowship of the Italian Ministry of Education. Since 1974, he has been an Assistant Professor of Microwaves at Rome University La Sapienza. He was also professore incaricato of Microwaves at the University of Catania, Catania, Italy, from 1975 to 1976, and of the University of Ancona, Ancona Italy, from 1976 to 1977. From 1977 to 1981, he was professore incaricato of Solid State Electronics at the University of Rome La Sapienza, where he is presently an Associate Professor of Microwave Measurements. From September to December 1983, he was appointed as a Research Fellow in the Electrical Engineering Department of the University of Texas at Austin, Austin, TX. His research activities have been concerned with electromagnetic wave propagation in anisotropic media, numerical solution of electromagnetic structures, electromagnetic field interaction with biological tissues, and mainly with the analysis and design of microwave and millimeter-wave integrated circuits.

Since 1978, Dr. Sorrentino has been a member of the Executive Committee of the IEEE Middle and South Italy Section, and is the Chairman of the local MTT Chapter. He is also a member of the Italian Electrical Society (AEI).